J Mater Sci (2008) 43:3867–3872
DOI 10.1007/s10853-007-2338-7

Atomistic study of the effect of B addition in the FeAl compound

J. M. Raulot · A. Fraczkiewicz · T. Cordonnier · H. Aourag · T. Grosdidier

Received: 6 July 2007 / Accepted: 20 November 2007 / Published online: 6 March 2008

Abstract First principle calculations have been carried out to study energetic of boron atom impurities in bulk and symmetric Σ5(310) tilt grain boundaries of the ordered stoechiometric B2 FeAl intermetallic. A set of configurations was considered for studying the bulk behaviour: B in tetrahedral and octahedral interstitial positions or substituting Al and Fe. For the analysis of the segregation at the grain boundary, calculations were done for B substituting Al and Fe at three different locations and for B filling empty spaces along the interface. In each case, the defect formation energies were calculated to determine the site preference and their relative stability. The results indicate that B doping is metastable in the bulk and tends to segregate along the grain boundary. The overall behaviour of the B atoms at the boundary is essentially driven by the strong Fe–B interactions.

Introduction

Iron-rich aluminides are potential candidates for a wide range of applications as high-temperature structural materials for magneto-electronic, automotive and power production industries. It is well known that iron–aluminide alloys exhibit limited strength and creep resistance at high temperature and low ductility at room temperature. The introductions of a second phase as precipitate or doping by B atoms are common practices used to improve these weaknesses. Several theoretical and experimental works have demonstrated that the mechanical and embrittlement properties can be improved by small addition of boron and 3d-4d transition metallic elements [1–9]. For example, FeAl alloys present an intrinsic intergranular brittleness in their 'pure' state and change their fracture mode, when boron-doped, towards a less brittle fracture taking place in a transgranular manner [10–12].

Several theoretical studies based on first principles calculations have already concentrated on determining the stability and the nature of the defects present in FeAl intermetallic compounds [13–17]. In the case of B doping, the B atom has only been studied as interstitial on octahedral sites [18, 19] or as a substitute to Fe and Al atoms [17, 20] but the insertion on tetragonal sites has been ignored. Furthermore, the effect of the B atom at grain boundaries has not been studied in FeAl using the high potential of ab-initio calculations. Therefore, the aim of this article is to gain new insights on the effect of B atoms in FeAl intermetallics, including the study of B on tetrahedral sites and at sigma 5 (310)[001] type of grain boundary.

Methods

Computational method

Calculations based on the density functional theory (DFT) [21, 22] have been carried out using the Vienna ab initio software package (VASP) [23–27]. The Vanderbilt

J. M. Raulot (✉) · T. Grosdidier
Laboratoire d'Etude des Textures et Applications aux Matériaux (LETAM), UMR-CNRS 7078, Université Paul Verlaine de Metz, Ile du Saulcy, 57042 Metz, France
e-mail: raulot@univ-metz.fr

A. Fraczkiewicz · T. Cordonnier
Centre de Sciences des Matériaux et des Structures, UMR CNRS 5146, ENSMSE, 158 Cours Fauriel, 42023 St Etienne, Cedex 2, France

H. Aourag
Laboratoire d'Etude et de Prédiction de Matériaux, URMER, Université de Tlemcen, 13000 Tlemcen, Algeria

Table 1 Pseudopotentials parameters used in the present work

Element	Fe	Al	B
Electronic configuration	$[Ar]3d^74s^1$	$[Ne]3s^23p^1$	$[He]2s^22p^1$
Kinetic energy cut-off (eV)	237	129	257
Atomic Wigner-Seitz radii (Å)	1.302	1.402	0.905

ultrasoft pseudopotentials [28] of the VASP library and a plane wave basis set were used for the calculation. The pseudopotentials were generated within the framework of the gradient-conjugated approximation (GGA) [29] to describe the exchange correlation energy. In the pseudopotential approach, the core electrons that do not participate in the atomic bonding are frozen and only the valence electrons are taken into account. The electronic configurations, the selected kinetic energy cut-off and the atomic Wigner-Seitz radii used to calculate the partial density of states are reported in Table 1.

A Monkhorst-Pack grid was used to sample the Brillouin zone [30]. The dimension of the k point grid varies with the cell size in order to keep a constant k point density in the Brillouin zone. In the pure FeAl compound, with a kinetic value of cut-off fixed at 240 eV and a grid of 84 points ($12 \times 12 \times 12$), the convergence of the total energy was close to 0.001 eV. The influence of different boron defects was analysed with periodic boundary conditions using a supercell containing 54 atoms ($3 \times 3 \times 3$ primitive cell). In this case, the *k* points grid of the supercell was $4 \times 4 \times 4$ (10 points). In some cases, comparison was also done with a supercell containing 16 atoms ($2 \times 2 \times 2$ primitive cell). The grid was modified in the case of the grain boundary studies in order to conserve the *k* points density.

Among the different convergence tests performed to assess the energy cut-off of FeAl, some comparisons were done with 240 and 350 eV as energy cut-off. The difference in energy convergence between the two cases was lower than 0.005 eV. The selected kinetic energy cut-off was 280 eV in the supercell when a boron atom was added.

The calculation was semi-relativistic and the spin polarisation was taken into account for the all the calculations. Only the ferromagnetic cases were considered because the iron ferromagnetic case was the most stable.

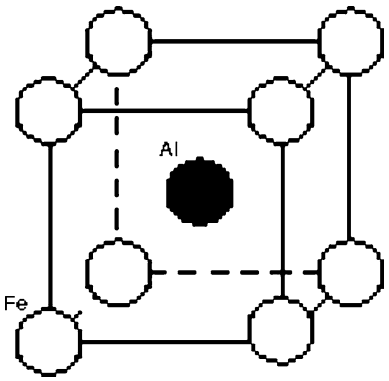

Fig. 1 B2 structure of the FeAl compound

All the structures have been relaxed using a conjugate gradient algorithm. Both the atomic position and supercell volume have been optimised. After relaxation, the forces on the atoms were checked to be lower than 0.02 eV/Å and the external pressure lower than 0.5 kB.

Simulation boxes

The FeAl compound has a B2 structure (space group 221, prototype CsCl, person symbol cP2) where the cell is cubic and the coordinates of the iron and Al atoms are (0,0,0) and (0.5,0.5.0,5), respectively. This is represented in Fig. 1. The selected system size (number of atoms) used for the calculations is a compromise between accuracy and computing cost. A "supercell" of $3 \times 3 \times 3$ B2 cubic cells consisting of 54 atoms in total was used to study the effect of B in the bulk. The cell has the following lattice vectors (3a,0,0), (0,3a,0), (0,0,3a), and both the atomic positions and the supercell volume have been optimised. For the case of B segregating at sigma 5 (310)[001] boundaries, a cell configuration consisting of a total of 36 Fe and Al atoms was used. In order to simulate a structure with defect, an extra impurity atom of boron was placed within the supercells.

For the bulk analysis, three different types of structural defects were investigated. In the first configuration (Fig. 2a), the interstitial impurity atom was placed on the

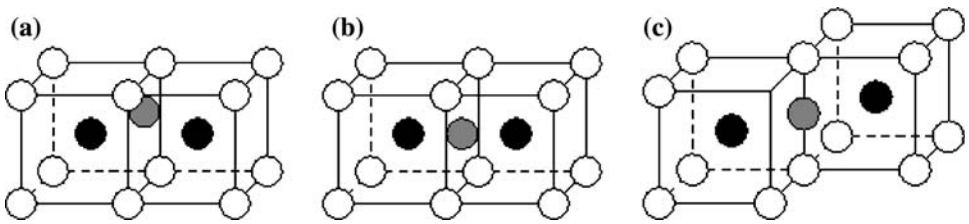

Fig. 2 Schematic of the three boron insertion configurations in the B2-FeAl structure: (**a**) boron atom in a tetrahedral position having 2Fe and 2Al atoms first neighbours (Bi tetra). (**b**) boron atom in an octahedral position with 2Al atoms as first neighbours (Bi octa Al), (**c**) boron atom in an octahedral position with 2Fe atoms as first neighbours (Bi octa Fe)

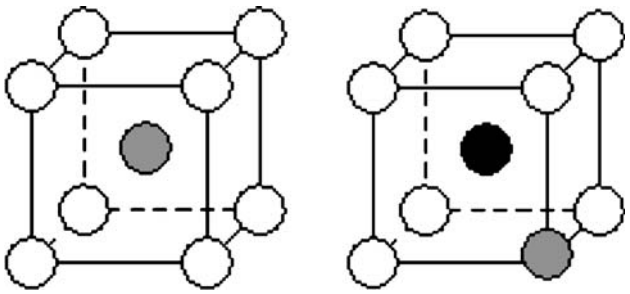

Fig. 3 Schematic of the two substitution configurations: boron atom (in grey) substituting (**a**) an Al atom (B_{Al}) and (**b**) a Fe atom (B_{Fe})

tetrahedral site ($B_{i\ tetra}$) of the B2 lattice. In the second one (Fig. 2b and c), the impurity atom was placed at octahedral positions (i.e. at the middle of the cubic cell and at the middle of the edge). The octahedral configuration allows two different positions: (i) the B atom placed between two aluminium atoms as first neighbours ($B_{i\ octa\ Al}$—Fig. 2b) or (ii) between two first neighbour atoms ($B_{i\ octa\ Fe}$—Fig. 2c). The third configuration is the substitution of a metallic atom by the B impurity. Again, this generates two possibilities: (i) B replacing Al and having iron as first neighbours B_{Al} (Fig. 3a) and (ii) B replacing an Fe atom (Fig. 3b).

The simulation of the Σ5 grain boundaries was done within the CSL (Coincidence Site Lattice) scheme. Figure 4 shows the simulation cell with its (310) interfacial plane. In this case, 18 atomic planes were needed to obtain sufficient separation between the two cell boundaries and, thereby, reasonable energy convergence. This has lead to a total of 36 atoms. In Fig. 4, the simulation cell used is viewed along the [001] direction and the different empty

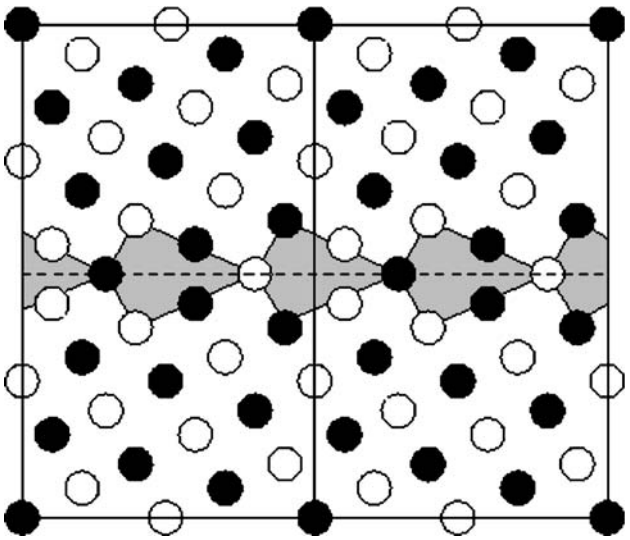

Fig. 4 Schematic of the sigma 5 grain boundary with the (310) interfacial plane

positions used to place impurities are highlighted. The cell containing the 36 atoms has following lattice vectors ($\sqrt{10}$ a,0,0), (0, $N\sqrt{10}/6 \sin\alpha$,0), (0,0,a). N is the number of planes, α is the angle of misorientation (36.87° for the sigma 5 (310)). Both the atomic positions and the supercell volume have been optimised for the calculations.

Formation energies

The formation energy of a defect was calculated using the procedure described in [31, 32].

For the boron atom in insertion, the following reaction way is considered:

FeAl (solid) + B (solid) → FeAl + B (solid).

In this case, the formation energy is given by: $E_F = E^{solid}_{FeAl+B} - E^{solid}_{FeAl} - E^{solid}_{B}$, where E^{solid}_{FeAl+B} is the energy of the supercell with a boron atom (16 or 54 atoms with one boron atom), E^{solid}_{FeAl} is the energy of the supercell without the defect and (16 or 54 atoms 50% iron and 50% aluminium) E^{solid}_{B} is the energy of one boron atom in the rhombohedral structure (cell with 12 atoms).

For substitution, the following reactional way is considered:

FeAl (solid) + B (solid) → FeAl + B (solid) + Fe or Al (solid).

The formation energy associated is $E_F = E^{solid}_{FeAl+B} + E^{solid}_{Fe\ or\ Al} - E^{solid}_{FeAl} - E^{solid}_{B}$, where $^{solid}_{Fe\ or\ Al}$ is the energy of one atom of Fe or Al depending on which atom is replaced (the cell of Al or Fe pure has one atom).

The number of atoms transferred from the supercell to the reservoir (B solid or Fe/Al solid) in order to create the defect is one. To maintain the accuracy by error cancellation, the energies are computed with the same grid of k points and the same kinetic energy cut-off values for the same supercell size.

Results and discussion

Bulk

Table 2 gives the calculated lattice parameter together with the energy of convergence, the k points and energy cut-off values that were used in the case of the bulk FeAl B2 structure without any defect. For comparison, in Table 2, is also given the experimental lattice parameter.

The structure was optimised by the relaxation of the lattice parameter in order to minimise the forces and the stress tensor. At the most, the a parameter is only approximately 0.5% different from the experimental one. The data in Table 2 also show that there is no or very

Table 2 Lattice parameter and convergence energy in the primitive FeAl cell

Optimization B2 FeAl				
	Energy by motif (eV)	*k* points	Ecut (eV)	*A* (Å)
This work	−12.590	8 × 8 × 8	240	2.8759
	−12.593	15 × 15 × 15	240	2.8759
	−12.589	15 × 15 × 15	350	2.8774
Experimental [33]				2.862

limited effects when modifying the *k* points and Ecut values within the range used in the present work. The different parameter modification yields a volume error of 2% or less, which is within the error usually obtained with DFT methods.

Concerning the supercell doped by boron atoms, the structure was optimised by alternatively repeating the relaxation of the ions in order to minimise the forces, the variation of the volume and the shape of the supercell to minimise the stress tensor. The values of the energy of the various defects within the grand-canonical framework formed with boron (Ed) are given in Table 3 together with their energy of formation. The Ed values obtained with a supercell of 54 atoms are quite consistent with the previously reported data given in [18, 19]. In addition, even when the cell size is reduced down to 16 atoms, the trends are nicely reproduced.

In terms of energy formation, all the energies are positive. This indicates that the energy of the system without defect is always lower than the energy of the system with a defect. In other words, none of these configurations with boron atom is energetically favourable in the bulk, which suggests that additional "perturbation" of the crystallographic structure should be required to stabilise the boron atom in this intermetallic. As will be discussed further hereafter, this can be done by the presence of dislocations and grain boundaries, for example. Among these "virtual" metastable configurations, the classification of the most favourable case to the least probable one is:

$$B_{Al} < B_{i\ octa\ Al} < B_{i\ octa\ Fe} < B_{Fe} < B_{i\ tetra\ Fe}.$$

The energy maximum is for the configuration where B is on a tetrahedral site. Modelling showed that a relative maximum point exists for the atomic migration of the B atom. This point is located halfway between the two types of octahedral sites. Despite this high energy value at 2.06 eV corresponds to a local minimum because the boron atom was found to be stable at the centre of the tetrahedral site. The migration energy must be higher than the energy difference between the octahedral and the tetrahedral configurations: 0.70 eV on the $B_{i\ octa\ Al}$ side and 0.18 eV on the $B_{i\ octa\ Fe}$ side.

The lattice parameter associated with the different types of B defects together with their relative variation with respect to the configuration corresponding to the bulk, defect-free FeAl structure are given in Table 4.

In terms of cell size, the variations in lattice parameter are always rather small, less than 0.6%. However, the trends are very clear. The data indeed indicate that the substitutions of Fe and Al by B create a contraction while inserting a B atom on an interstitial site creates an expansion of the lattice. The highest amount of expansion is obtained for B inserted on a tetrahedral site.

Grain boundary without defect

The sigma 5 (310) structure was optimised for different number of crystallographic planes separating the grain boundaries. Table 5 gives the calculated surface energy as a function of the number of separating planes.

The interface energy, γ, was calculated using the following expression:

$$\gamma = \frac{E_{FeAl}^{interfaces} \quad E_{FeAl}^{volume}}{2S_{interfaces}}$$

Table 3 Formation energies of Boron defect and grand canonical defect energies (Ed) in eV

Boron defects							
		$B_{i\ octa\ Al}$	$B_{i\ octa\ Fe}$	$B_{i\ tetra}$	B_{Al}	B_{Fe}	Atom by supercell
Ed	Yan (LDA) [18]	−5.94	−5.09	–	−1.93	+1.42	136
	Besson (SGGA) [19]	−5.88	−4.92		−2.54	+3.54	54
	This work (SGGA)	−4.52	−4.67	−4.18	−1.62	+3.62	16
	This work (SGGA)	−5.34	−4.82	−4.64	−2.47	+3.64	54
$E_{formation}$	Yan (LDA) [18]	+0.97	+0.12	–	0.00	+0.11	136
	This work (SGGA)	+2.18	+2.03	+2.52	1.38	+2.02	16
	This work (SGGA)	+1.36	+1.88	+2.06	0.54	+2.03	54

Table 4 Lattice parameters associated with the different types of B defects and their relative variation compare to a defect-free FeAl structure

Type of boron associated defect						
	$B_{i\ octa\ Al}$	$B_{i\ octa\ Fe}$	$B_{i\ tetra}$	B_{Al}	B_{Fe}	FeAl
a_0 (A)	2.891	2.892	2.895	2.869	2.872	2.878
Δa_0 (%)	+0.44	+0.49	+0.59	−0.33	−0.24	0

Table 5 Interface energies convergence test carried out with the (4 × 2 × 9) *k*-points grid

Interface energies γ_s (J/m^2)	
Atomic planes between two grain boundaries	Σ5(310)[001]
5	1.149
7	1.128
9	1.124

where $E_{FeAl}^{interfaces}$ is the energy of the FeAl with two grain boundaries by cell, E_{FeAl}^{volume} is the energy of the FeAl compounds without defect and $S_{interface}$ is the dimension of the interface. We can observe that the interface energy converge quite rapidly. Therefore, for the B free structure the configuration with nine crystallographic planes between two grain boundaries can be considered.

Grain boundary with Boron segregation

B atoms have been introduced at different locations along the grain boundary for the previously optimised cell size where nine crystallographic layers separated the grain boundaries in the simulation box. In this case of a fairly small supercell (nine planes), a small distortion occurred at the opposite grain boundary that was not doped with B. To avoid this effect, calculations were also carried out using a supercell having 20 planes between the adjacent grains boundaries. In this case, to avoid extremely long calculation times, only the gamma point was used to represent the *k* points (1 × 1 × 1 instead of 4 × 2 × 9). The details of the calculation are recalled in Table 6 together with the different results of energy formation (E_F) obtained for the different B atom locations studied. The calculations were done for B substituting Al and Fe at different locations along the interface as well as for B filling empty spaces where the free volume is important. The different configurations are shown in Fig. 5. They consist of three substitutions of Al atoms (marked Al1 to Al3—black atoms), three substitutions of Fe atoms (marked Fe1 to Fe3—white atoms) and two insertions at the boundaries for which the B atom is either surrounded by Fe near-neighbour atoms (Insertion 1) or Al ones (Insertion 2).

For the insertion and substitution cases respectively, the formation energy of the boron defects in the grain boundary are the following:

$E_F^{GB} = E_{FeAl+B}^{GB} - E_{FeAl}^{GB} - E_B^{solid}$ for the energy of an insertion defect, and

$E_F^{GB} = E_{FeAl+B}^{GB} + E_{Fe\ or\ Al}^{solid} - E_{FeAl}^{GB} - E_B^{solid}$ for the energy of a substitutional defect, where E_{FeAl}^{GB} and E_{FeAl+B}^{GB} are the energies of a grain boundary without and with a boron defect.

The results for the six possible substitutions and two insertions along the sigma 5 (310) boundary are given in Table 6. Except for the case of the Fe2 substitution, the results of the calculations done using 9 or 20 planes in the simulation box give the same general trends. In the case of

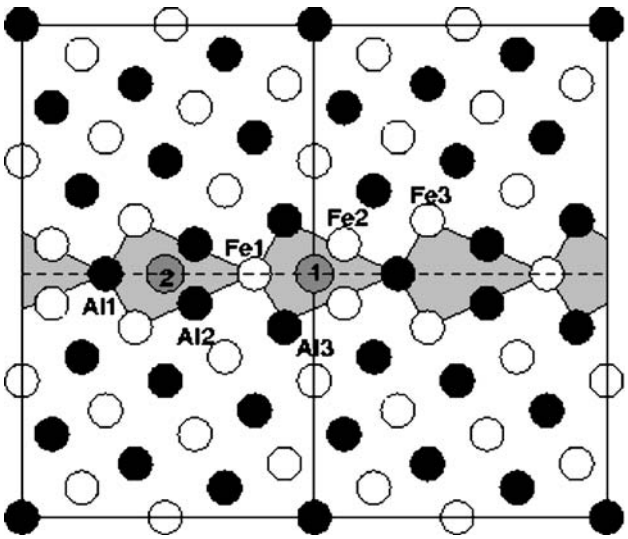

Fig. 5 Visualisation of the possible doped boron sites in the sigma 5 grain boundary with the (310) interfacial plane

Table 6 Formation energy of a boron defect in a sigma 5 (310) grain boundary

Boron defects in the sigma 5(310)										
Positions	Planes	*k* points	Insertion 1	Insertion 2	Al1	Al2	Al3	Fe1	Fe2	Fe3
E_F (eV)	9	4 × 2 × 9	−1.53	−0.30	1.16	−1.29	0.51	1.39	−0.50	0.47
E_F (eV)	20	1 × 1 × 1	–	–	1.02	−0.22	0.12	1.24	1.36	1.05

Fe2 substitution the change in trend are associated with a fairly strong modification of the self consistent calculation, which is more precise for this highest atomic plane (20 planes). Thus, it is clear that the substitution of Fe by B is never favoured when compared to substituting an Al atom. Among the different substitution configurations, the Al2 configuration is the most favourable. In this case, the B atom substituting Al becomes surrounded by three Fe near-neighbours. The presence of these Fe-B bindings is the reason for the higher stability of this configuration. It has indeed been demonstrated recently that Fe–B interactions are much more important than Al–B ones when the B atom is located on an Al site [20]. Other favourable configurations are the insertion of the B atom within the empty spaces left along the Σ5 boundary. Again, this is particularly true when Fe near neighbours surround the B atom such as the case "Insertion 1".

Conclusion

Ab initio calculations have been carried out to depict the behaviour of B atoms in the bulk and at symmetric Σ5(310) tilt grain boundaries of the ordered stoichiometric B2-FeAl intermetallic compound. The main results are as follows:

- In the bulk, 0.50 eV must be given to stabilise a B_{Al} (substitution) defect and the insertion of B at tetragonal sites is the least possible case.
- The lattice parameter decreases when the boron atom is on a substitution site (volume effect), and increases when the boron atom is on an insertion site.
- A boron atom in the bulk is metastable and tends to segregate as an interstitial or a substitutional (for Al) impurity along the grain boundary.
- The interface energy in a symmetric Σ5(310) tilt boundaries of the ordered stoichiometric B2-FeAl compound has been established to be 1.12 J/m^2 in the B-free system.
- At the grain boundary, the favoured configurations are those that create Fe-B interactions very close to the theoretical boundary. Therefore, for a Σ5(310) tilt boundary, only two configurations are favoured out of the eight possible ones.

References

1. Fraczkiewicz A, Gay A-S, Biscondi M (1998) Mater Sci Eng A 258:108
2. Gay A-S, Fraczkiewicz A, Biscondi M (1999) Mater Sci Forum 294–296:453
3. Morris DG, Morris-Munoz MA (1999) Intermetallics 7:1121
4. Radhakrishna A, Baligidad RG, Sarma DS (2001) Scripta Materialia 45:1077
5. Banerjee R, Amancherla S, Banerjee S, Fraser HL (2002) Acta Materialia 50:633
6. Bozzolo GH, Noebe RD, Amador C (2002) Intermetallics 10:149
7. Mekhrabov AO, Akdeniz MV (1999) Acta Materialia 47:2067
8. Medvedeva NI, Gornostyrev YuN, Novikov DL, Mryasov ON, Freeman AJ (1998) Acta Materialia 46:3433
9. Munroe PR, Kong HC (1996) Intermetallics 4:403
10. Calonne O, Fraczkiewicz A, Louchet F (2000) Scripta Materialia 43:69
11. Baker I, Li X, Xiao H, Carleton R, Georg EP (1998) Intermetallics 6:177
12. Deevi SC, Sikka VK, Inkson BJ, Cahn RW (1997) Scripta Materialia 36:899
13. Mayer J, Fahnle M (1997) Scripta Mater 37:131
14. Bozzolo G, Ferrante J, Noebe RD, Amador C (1997) Scripta Mater 36:813
15. Krachler R, Ipser H (1999) Intermetallics 7:141
16. Faupel F, Hehenkamp Th (1999) Intermetallics 7:289
17. Kellou A, Feraoun HI, Grosdidier T, Coddet C, Aourag A (2004) Acta Mater 52:3263
18. Yan J-A, Wang C-Y, Wang S-Y (2005) Phys Rev B 72:134108
19. Besson R, Legris A, Morillo J (2002) Phys Rev Lett 89:225502
20. Kellou A, Grosdidier T, Aourag H (2006) Intermetallics 14:142
21. Hohenberg P, Kohn W (1964) Phys Rev 136:B864
22. Kohn W, Sham L (1965) Phys Rev 140:1133
23. Hafner J (2000) Acta Mater 48:71
24. Kresse G, Hafner J (1993) Phys Rev B 47:558; (1994) 49:14251
25. Kresse G, Furthmüller J (1996) Phys Rev B 54:11169
26. Kresse G, Furthmüller J (1996) Comput Mater Sci 6:15
27. Kresse G, Hafner J (1996) J Phys Condens Matter 6:8245
28. Vanderbilt D (1990) Phys Rev B 41:7892
29. Perdew JP, Wang Y (1991) Phys Rev B 45:13244
30. Monkhorst HJ, Pack JD (1976) Phys Rev B 13:5188
31. Zhang SB, Wei SH, Zunger A, Katayama-Yoshida H (1998) Phys Rev B 57:9642
32. Wei SH, Zhang SB, Zunger A, Katayama-Yoshida H (1999) J Appl Phys 85:7214
33. Villars P, Calvert LD (1986) Pearson's handbook of crystallographic data for intermetallic phases. American Society for Metals, Metals Park